Coral Reefs
https://doi.org/10.1007/s00338-025-02637-6

REPORT

Growth and ontogenetic change in juvenile crown-of-thorns sea star (*Acanthaster* sp.) morphology: Can morphometrics be used as an aging tool?

Liam J. Wilson[1] · Thomas E. White[1] · Miles Lamare[2] · Paulina Selvakumaraswamy[1] · Maria Byrne[1]

Received: 9 August 2024 / Accepted: 17 February 2025

Abstract The crown-of-thorns sea star (COTS, *Acanthaster* sp.) is a coral predator that, in population outbreaks, causes major coral loss in Indo-Pacific reefs. Current paradigms explaining the cause of outbreaks focus on the larval and adult stages, while the early herbivorous juvenile stage remains a black box in our understanding of COTS. We followed growth in a large laboratory population of juveniles from settlement to 300 days. Ontogenetic changes in eight traits over time were quantified, including those typically used to track growth in sea stars (total diameter, arm number) and traits not previously quantified (e.g. spine number/type). Combinations of traits were modelled against age to explore their potential as indicators of age. Total diameter exhibited a strong association with age, as did covarying traits: central disk diameter, mouth diameter and arm length. The number of pointed spines was also strongly associated with age, greater in association than arm number. Our results indicate that use of a combination of morphological traits has potential as an indicator of juvenile age. In particular, pointed spines appear to have potential as an age marker for juveniles. Using size-at-age data, we investigated the fit of growth models to estimate age-size relationships. A Gompertz model provided the best fit to the growth/age data and is consistent with the size/time of diet shift (herbivory to corallivory) in juvenile COTS. Addressing knowledge gaps on these juveniles to inform age modelling using morphological traits contributes to the understanding of the biology and ecology of this cryptic life stage.

Keywords *Acanthaster* · Herbivorous juveniles · Growth traits · Age modelling

Introduction

Coral reefs are highly diverse habitats and are one of the world's most threatened ecosystems due to their vulnerability to climate change and local stressors (Hughes et al. 2017; Byrne et al. 2024a). With over a decade of global mass bleaching events, it is clear that marine heatwaves are the major cause of coral mortality with dire prospects for the future of coral reefs (Hughes et al. 2017; Bozec et al. 2022). As a major local and regional stressor, Indo-Pacific coral reefs are also impacted by outbreaks of the coral-eating crown-of-thorns sea star (COTS; *Acanthaster* sp.) (Deaker and Byrne 2022; Pratchett et al. 2014). These outbreaks differ from climate warming in that they are somewhat amenable to management interventions. Control programs are the main direct action for managers, with considerable financial investment into COTS monitoring and killing programs (GBRMPA 2017; Plagányi et al. 2020).

Acanthaster species exhibit boom-and-bust population dynamics (Uthicke et al. 2009) that are likely to be a natural facet of their ecology (Deaker and Byrne 2022; Vine 1973). At low densities, COTS have low impact on the coral community and are suggested to enhance diversity by creating space that can be colonised by faster growing coral species (Colgan 1987; Done and Potts 1992). In contrast, high-density populations can drastically alter coral communities

Supplementary Information The online version contains supplementary material available at https://doi.org/10.1007/s00338-025-02637-6.

✉ Liam J. Wilson
liam.wilson@sydney.edu.au

[1] School of Life and Environmental Sciences, The University of Sydney, Sydney, Australia

[2] Department of Marine Science, University of Otago, Dunedin, New Zealand

Published online: 06 March 2025

threatening reef function and diversity (Kayal et al. 2012; Pratchett et al. 2014).

Several hypotheses, largely focused on larval and adult stages, have been proposed to explain COTS outbreaks. The terrestrial runoff/nutrient enrichment hypothesis posits that elevated nutrients from eutrophic runoff stimulate increases in phytoplankton food for larvae, enhancing their success (Birkeland 1982). However, the link between runoff events and COTS outbreaks is equivocal (Kroon et al. 2023; Pratchett et al. 2014; Wolfe et al. 2017). The overfishing/predator removal hypothesis posits that adult COTS have been released from predator control (Endean 1969; Kroon et al. 2021). Recent research points to the role that reservoirs of juveniles may have in driving outbreaks, the juveniles-in-waiting hypothesis (Deaker et al. 2020a; Wolfe and Byrne 2024). Given the inherent traits of COTS and plasticity across life stages (Deaker and Byrne 2022), it is likely that many interacting factors across COTS life stages influence outbreaks.

Acanthaster begin their benthic life as herbivores. These juveniles are cryptic in the reef infrastructure and are difficult to study (Wilmes et al. 2018, 2020a, b). They feed on crustose coralline algae (CCA) as their preferred food but can subsist on algal films (Deaker et al. 2020b; Lucas 1984; Yamaguchi 1973). The juveniles can remain as herbivores for at least 6.5 years in the absence of coral prey (Deaker et al. 2020a). Over multiple recruitment events, cohorts of juveniles have the potential to accumulate as a "hidden army" in the reef infrastructure until suitable conditions manifest, serving as a proximate source of outbreaks. In situations of low coral prey such as after bleaching events or COTS outbreaks, these cryptic juveniles may persist for some time (Byrne et al. 2023; Wolfe and Byrne 2024). A delayed switch to the adult diet and habitat occurs in other predatory sea stars, potentially influenced by density dependent feedback (Byrne et al. 2021; Nauen 1978). For juvenile COTS, the switch to corallivory may be influenced by interference competition/semiochemicals from conspecific adults (Webb et al. 2024). The inability to target COTS across its benthic phases in mitigation/control programs emphasises the need for increased knowledge of the juvenile stage.

The timing and size at which the diet shift to corallivory occurs varies among juveniles and depends on availability of preferred coral prey, as well as the risk of sublethal predation/damage from coral tentacles (Deaker et al. 2021a; Johansson et al. 2016; Lucas 1984; Neil et al. 2022; Wilmes et al. 2020a; Yamaguchi 1974; Zann et al. 1987). Juvenile COTS can transition to a coral diet as early as four to six months of age and 8–10 mm diameter (Lucas 1984; Yamaguchi 1974). On an algal diet in the absence of coral prey, juveniles reach a maximum size of 16–18 mm diameter followed by years-long growth stasis (Deaker et al. 2020b). In nature, the size of juvenile COTS at the diet switch to corals is highly variable (Zann et al. 1987; Wilmes et al. 2020a). In situ studies have found large juveniles on CCA (10–32 mm diameter) (Zann et al. 1987; Wilmes et al. 2020a). When the juveniles become coral predators, they grow quickly (Yamaguchi 1973, 1974; Lucas 1984; Zann et al. 1987; Birkeland and Lucas 1990). The age-size disconnect of juvenile COTS, where the age of individual juveniles cannot be discerned from their size, presents a challenge to modelling growth. Unless cohorts are monitored from settlement, the plasticity of growth in response to environmental conditions complicates the aging of juvenile echinoderms (Byrne et al. 2021).

The ontogenetic changes in juvenile COTS from the 5-armed stellate to the multiarmed disk morphology is described in Byrne et al. (2024b). Given their remarkable growth plasticity, a detailed assessment of their growth is needed. To document their development and transition to a coral diet, juvenile COTS have been reared in laboratory studies (Deaker et al. 2020a, b; Johansson et al. 2016; Lucas 1984; Neil et al. 2022; Yamaguchi 1973, 1974). Two of these studies documented growth from metamorphosis through the herbivorous juvenile stage using changes in total diameter and arm number as metrics (Yamaguchi 1973, 1974; Lucas 1984). Yamaguchi (1973) followed the growth of 14 juveniles for five months and Lucas (1984) documented development of 6 herbivorous stage juveniles for over a year.

We built on previous rearing studies (Yamaguchi 1973, 1974; Lucas 1984; Byrne et al. 2024b) in documenting development of a large laboratory population of juveniles from settlement and metamorphosis to the advanced herbivorous juvenile. Studies on juvenile COTS have used the number of arms and diameter as individual traits to characterise growth (Deaker et al. 2020a, b; Lucas 1984; Wilmes et al. 2020a; Yamaguchi 1973, 1974; Zann et al. 1987). However, as single-trait growth markers, their application is limited in advanced juveniles because diameter reaches growth stasis on an algal diet (Deaker et al. 2020a) and the number of arms reaches a maximum with no subsequent additions to mark growth (Yamaguchi 1973). In addition to these two traits, we quantified ontogenetic change in traits not previously quantified (e.g. spine type, number) over time in juveniles of known age, from settlement to 300 days age. We sought to identify markers/traits either individually or in combination that varied regularly over time as used in aging methods for other marine invertebrates (Peharda et al. 2018; Sun et al. 2019).

An ability to age juvenile COTS using morphological traits would greatly enhance our understanding of their biology and post-settlement processes, as well as the potential of cohorts of juveniles to generate outbreaks. In a model test approach, we addressed the hypothesis that a suite of combined traits might be useful to determine the age of COTS juveniles. Using our size-at-age data, we also investigated

the fit of growth models to describe age-size relationships of the juveniles.

Methods

Juvenile rearing

As the taxonomy of the Pacific species of *Acanthaster* is uncertain (Haszprunar et al. 2017), we use *Acanthaster* sp. or COTS to refer to the species investigated here. Adults were collected near Cairns (northern Great Barrier Reef–GBR) and shipped to the Sydney Institute of Marine Science where they were maintained in flow-through aquaria supplied with filtered sea water (FSW 5.0 µm) at 26–27 °C, the sea surface temperature of the Northern GBR (AIMS 2023). Small pieces of ovary and testis were dissected from the animals. The ovaries were placed in 10^{-5} M 1-methyl adenine in FSW to obtain fertile eggs. In two separate fertilisations, the eggs of two females and two males were combined to establish larval cultures using routine methods (see Clements et al. 2022). Larvae were reared in aerated 1L beakers of UV sterilised 1 µm FSW at 25–26˚C in a constant temperature (CT) room and fed *Proteomonas sulcata* (20,000 cells mL^{-1}) every two days. When they reached the competent brachiolaria stage (16 days post-fertilisation), settlement was induced using coralline algae, *Amphiroa* sp. The juveniles were then reared in the CT room (25–26 °C) in UV sterilised 1 µm FSW and fed small pieces of *Amphiroa* sp. Juvenile COTS grow well on this alga (Deaker et al. 2020b) and were fed ad libitum. They were initially placed in individual wells (5 mL) in 12-well culture dishes where they were reared up to ~ 3 mm diameter and then moved to wells (10 mL) in 6-well dishes. As the juveniles grew, they were moved into small plastic Petri dishes (10–20 mL) and then large glass (150–250 mL) dishes. Food and FSW were renewed every 3 days, while culture dishes were replaced weekly.

Photomicroscopy

Juveniles were haphazardly selected (n = 25–35 per ~ 30 days, 7–300 days) from a population of 110–150 individuals and were photographed using an Olympus dissecting microscope with an attached DP23 digital microscope camera and Olympus CellSens software (Figs. 1, 2). During the study, the number of juveniles available reduced due to mortality and the use of some individuals for other experiments. Prior to photography, the juveniles were relaxed in a 1:1 solution of FSW and 7% $MgCl_2$ for a short period, then returned to rearing conditions. Newly settled juveniles (1 week old) were photographed while attached to the algae to avoid disturbing them. In total, ~ 1250 photographs were used for this study. The photos were analysed using ImageJ (v1.53 k), with eight traits measured (Fig. 2): total diameter (arm tip to arm tip, hereafter diameter), disk diameter, mouth diameter, arm length (from the oral side) and the number of arms, arm buds, pointed spines, and marginal spines). Arm length and the number of pointed and marginal spines were measured using the three longest arms and the mean datum was used for analysis. Diameter and arm number have been used in previous studies of COTS juveniles (Lucas 1984; Wilmes et al. 2020a; Yamaguchi 1973, 1974) allowing comparison with the present study. Data for some traits (pointed spines, marginal spines, mouth diameter, disk diameter, arm length) were not assessed in the smallest juveniles (≤ 60 days) as they were not present or were difficult to resolve (e.g. pointed spines, disk diameter) and to reduce handling of the very small juveniles (e.g. oral side images, mouth diameter).

Statistical analyses

Trait data analysis

Trait data analyses were carried out using R version 4.3.3 (R Core Team 2024). Trait change over time was analysed for individual traits and we also explored if multiple traits could be used to model the age of COTS juveniles.

Univariate generalised additive mixed models (GAMMs) were fit using the 'mgcv' package 1.8.41 (Wood 2011) to explore the effect of time (the single smooth term predictor) on each of the eight morphological traits individually (trait ~ age). These models do not constrain age-trait relationships to the shapes of pre-specified parametric classes (Yee and Mitchell 1991), allowing the data to determine the shape of the response curve. Where traits exhibited a linear relationship with time (indicated by GAMM-estimated effective degrees of freedom ~ 1), linear mixed effect models (LMMs) were instead fit to the data with the morphological traits as the response variable.

The global dataset contained some repeated measures. Thus, juvenile ID was modelled as a random effect in both the GAMMs and LMMs (random intercept), and parameter estimates were obtained using maximum likelihood (ML). Smoothing was conducted using the penalised thin plate spline method (Wood 2003), with the basis dimension value (k) set to the minimum necessary to encapsulate the necessary dimensions of the underlying curve (Wood 2003), with a maximum value of 4 to avoid overfitting.

Initial data exploration revealed the number of arms exhibited under-dispersion. Thus, this trait was modelled using a quasi-Poisson error distribution with a log link function. All other traits were modelled using a Gaussian error distribution as the data were continuous.

The predicted values of GAMMs were plotted using the 'ggeffects' v1.2.2 (Lüdecke 2018) and 'ggplot2' v3.4.1

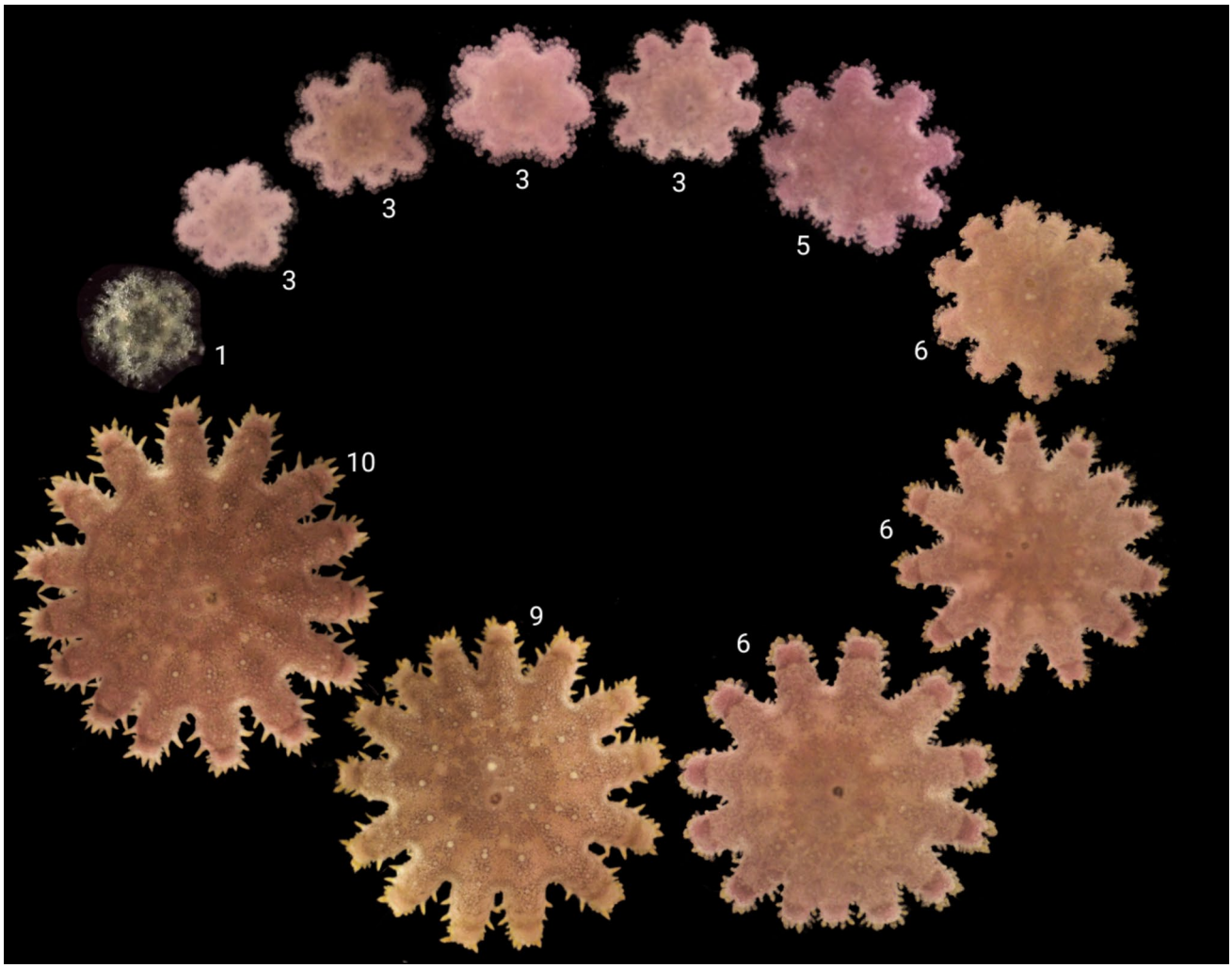

Fig. 1 Juvenile growth and arm addition. Numbers indicate age (months post-settlement). Juvenile sizes (clockwise from smallest) 0.82, 1.79, 2.16, 2.47, 3.32, 3.76, 3.76, 6.57, 6.34, 8.98 and 9.62 mm diameter, respectively

packages (Wickham 2016). Assumptions of normality of residuals and homoscedasticity were verified using the 'mgcv' package v1.8.41 (Wood 2011). Linear mixed effects models (LMMs) were also plotted using 'ggplot2' v3.4.1 (Wickham 2016). Assumptions of linearity, homoscedasticity, normality of residuals and normality of random effects were confirmed using the 'performance' package v0.10.2 (Lüdecke et al. 2021).

To explore if morphological change could be used to indicate juvenile age, we used data for the eight traits as predictors against age in multivariate LMMs. Correlation between traits was first examined using Kendall's τ-b, a measure that does not assume the relationship between variables is linear (Quinn and Keough 2002) and can account for ties in rankings arising from multiple observations of identical values (Togashi and Sakai 2019), which were observed in the data.

LMM assumptions of linearity, homoscedasticity, non-multicollinearity and normality of residuals and random effects were checked using the 'performance' package v0.10.2 (Lüdecke et al. 2021), with the variance inflation factor (VIF) used to assess collinearity. Whilst the VIF threshold used to indicate collinearity varies between studies (Quinn and Keough 2002), we used VIF ≥ 5 as the multicollinearity threshold to balance the stability of model parameter estimates with the risk of excluding variables of interest due to correlation.

Total diameter, central disk diameter, mouth diameter and arm length were highly correlated ($\sim\tau > 0.80$; Online Resource S1) and exhibited multicollinearity (VIF ≥ 5). As the total diameter trait (r) incorporates the central disk, mouth opening and arm length, we used total diameter as the proxy measure of individual size. Thus, we ultimately used five traits as predictors of age: total diameter, number

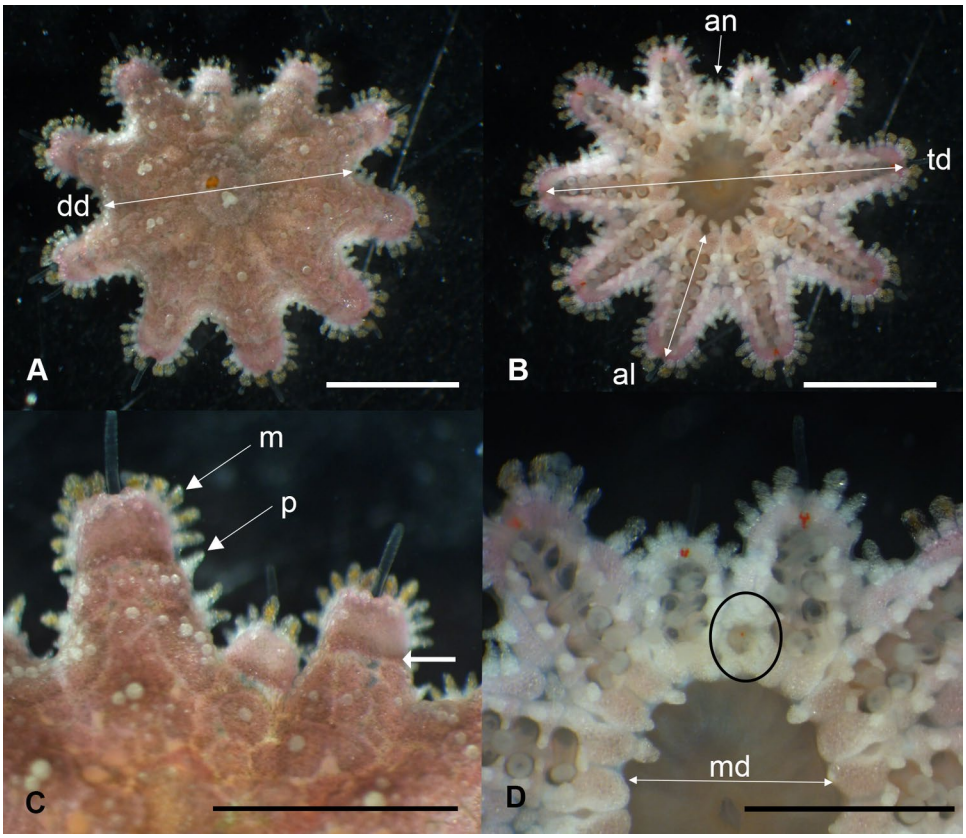

Fig. 2 Morphological traits in 180-day-old juveniles. **A, C** Aboral surface. **B, D** Oral surface. al, arm length; an, new arm; dd, disc diameter; m, marginal spine; md, mouth diameter; p, pointed spine; td, total diameter. Black circle, arm bud; white arrow, growth zone. Scale bars = 2 mm

of pointed spines, number of marginal spines, number of arm buds and number of arms. However, models containing both pointed spines and total diameter, as well as total diameter and the number of arms, exhibited multicollinearity and so these trait pairs could not be included in the same model. We therefore fit models using two trait sets: (1) total diameter, marginal spines and number of arm buds and (2) pointed spines, marginal spines, number of arms, and number of arm buds.

Using morphological traits as fixed effect predictors, multivariate linear mixed models were fit using the 'lmerTest' package v3.1.3 (Kuznetsova et al. 2017). Juvenile ID was modelled as a random effect and parameter estimates were obtained using ML estimation. Candidate models containing all subset combinations of the trait predictors were constructed and compared using Akaike information criterion (AIC) (in 'MuMIn' v1.47.5; Barton 2023). AIC_C, a small-sample modification of AIC, was used for comparison between models. Traits from the best-ranked model of each trait group were standardised to estimate the relative strength of effects of predictors on age (Schielzeth 2010; Siegel and Wagner 2022).

Growth modelling

We used the total diameter at age data over the first 300 days post-settlement to investigate the fit of four growth models (exponential, Gompertz, linear, logistic) to describe age-size relationships. Application of the Gompertz growth model follows recent application of this model for juvenile growth with age in COTS (Deaker et al. 2020a). For these analyses, we used data on the size of newly metamorphosed one week old (mean total diameter = 0.63 mm, SE = 0.02 mm, n = 29) juveniles. Curves were fit using the base 'stats' package v4.3.3 (R Core Team 2024), using a Gauss–Newton algorithm for nonlinear least squares analysis. Starting values were selected via visual inspection. Confidence intervals were calculated from predicted values obtained using 'investr' v1.4.2 (Greenwell and Schubert Kabban 2014). To determine the most appropriate growth model, model fit was compared using residual sum of squares (RSS) and visual inspection, as well as biological relevance in comparison with previous studies (Deaker et al. 2020a; Wilmes et al. 2020a). Growth curve analyses were carried out using R v4.3.3 (R Core Team 2024). For the Gompertz growth model, the best supported model, the age and size of inflection, the maximum growth rate and asymptotic size, were calculated. The exponential, linear and logistic growth models are presented in Online Resource S2.

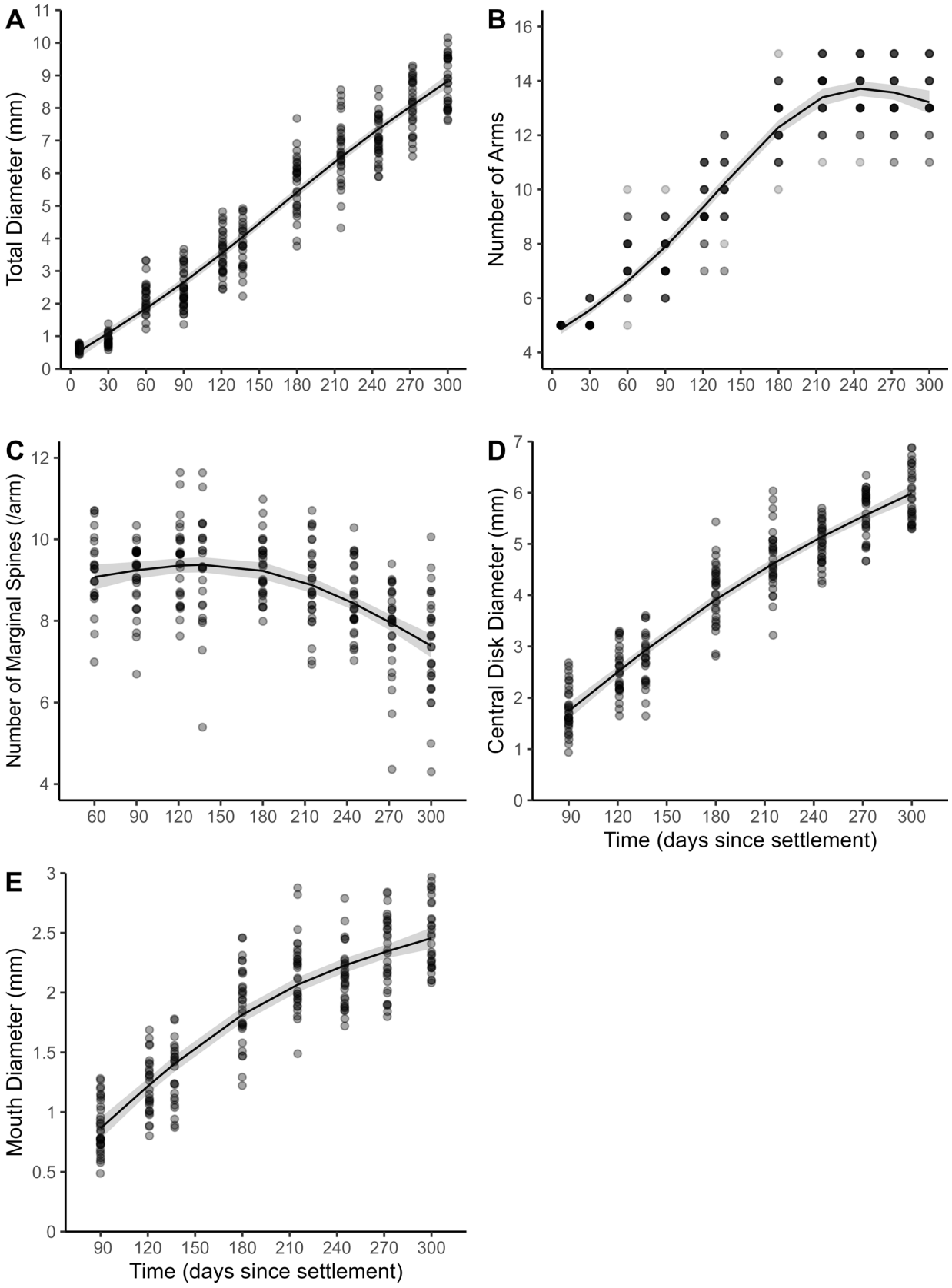
A
Total Diameter (mm)
0 1 2 3 4 5 6 7 8 9 10 11
0 30 60 90 120 150 180 210 240 270 300
B
Number of Arms
4 6 8 10 12 14 16
0 30 60 90 120 150 180 210 240 270 300
C
Number of Marginal Spines (/arm)
4 6 8 10 12
60 90 120 150 180 210 240 270 300
D
Central Disk Diameter (mm)
0 1 2 3 4 5 6 7
90 120 150 180 210 240 270 300
Time (days since settlement)
E
Mouth Diameter (mm)
0 0.5 1 1.5 2 2.5 3
90 120 150 180 210 240 270 300
Time (days since settlement)

◂**Fig. 3** GAMM plots of relationships between **A** total diameter, **B** the number of arms, **C** number of marginal spines per arm, **D** central disk diameter, **E** mouth diameter in juveniles to 300 days old. Points are individual observations ($n = 317$, 317, 263, 237 and 235 for total diameter, number of arms, marginal spines, central disk and mouth diameter, respectively). Data points are jittered to avoid over-plotting (one-day axis breaks; width = 0.15, height = 0). Grey shading, 95% confidence interval

Results

Ontogenetic changes in traits with age

The relationship between total diameter and age was marginally sigmoidal (edf = 2.62; Fig. 3a; Table 1) and it is likely that a distinct asymptote would have been reached if rearing had continued beyond 300 days (see Deaker et al. 2020a). At the beginning of the study, the week-old juveniles had a mean diameter of 0.63 mm (SE = 0.02, $n = 29$), increasing to 8.82 mm (SE = 0.14, $n = 30$) by 300 days age. The mean diameter of the juveniles at 90, 121, 137, 180 and 215 days post settlement was; 2.46 mm (SE = 0.10, $n = 34$, range 1.36–3.67 mm), 3.53 mm (SE = 0.12, $n = 29$, range 2.44–4.82 mm), 3.78 mm (SE = 0.15, $n = 25$, range 2.23–4.92 mm), 5.68 mm (SE = 0.16, $n = 30$, range 3.76–7.68 mm), 6.69 mm (SE = 0.18, $n = 30$, range 4.32–8.56 mm), respectively (Fig. 3a). The first juveniles reached the lower limit of the threshold to transition to corallivory (~ 8 mm diameter) at ~ 215 days.

At settlement, the juveniles had five arms (Fig. 1). One arm was on average added every 21.6 days (0.046 days/new arm) from 30 to 215 days old. Arm addition plateaued past this point (around seven months post-settlement) with a maximum number of arms of 15 (Fig. 3b). The relationship between time and the number of arms was approximately sigmoidal (edf = 2.96; Table 1).

The formation of a new arm was signalled by the appearance of an arm bud. After 30 days, the mean number of arm buds was 0.24 (SE = 0.09, $n = 25$). Only one arm bud was generally present at any one time (Fig. 2). As the bud grew to form a new arm, a new arm bud appeared between the two most recently formed arms. By 90 days post-settlement, the mean number of arm buds increased to 0.82 (SE = 0.07, $n = 34$), remaining steady through 137 days ($\bar{x} = 0.83$, SE = 0.08, $n = 24$). The number of arm buds declined as the maximum arm number was reached around ~ 215 days. No arm buds were observed from 245 days post-settlement.

At 90 days, the average arm length was 0.81 mm (SE = 0.04, $n = 34$, range 0.45–1.19 mm) with little variation among individuals (Fig. 4a). Arm length increased linearly with age (est. = 0.01 ± 0.0003, $df = 163.7$, $t = 36.663$, $p = < 0.001$, $n = 235$, $R^2_{Marginal} = 0.865$; Fig. 4a), reaching a mean of 3.19 mm by 300 days post-settlement (SE = 0.07, $n = 30$, range 2.49–3.87 mm).

The first spines that formed after metamorphosis were the fan-shaped (marginal) spines on the tips of arms, which function in attachment to the substratum (Figs. 2 and 5). The pointed spines appeared later and eventually dominated the surface. In the first ~ 245 days the marginal spines outnumbered the pointed spines and were the dominant spine type present in early juveniles (Figs. 2, 3c, 4b, and 5). The marginal spines were largely located at the tip of the arm distal to the growth zone band (Fig. 2) and were a translucent pink-white colour (Fig. 5). Marginal spines were occasionally observed on the sides of arms, growing off fleshy nodules on proximal regions of the arm. In juveniles ~ 3.5 mm diameter, the marginal spines began to take on a yellow-orange hue as the colour of the juvenile changed from translucent pink-white to pink-red. The number of marginal spines remained relatively unchanged in the early months before decreasing past ~ seven months post-settlement (Fig. 3c, Table 1). 60-day-old juveniles had an average of 9.22 (SE = 0.18, $n = 25$, range 7–10.67) marginal spines per arm and this was similar at 215 days ($\bar{x} = 8.91$, SE = 0.18, $n = 30$, range 7–10.67). These spines decreased by 300 days ($\bar{x} = 7.4$, SE = 0.23, $n = 30$, range 4.33–10).

From approximately six months of age, the pointed spines became more prominent and so the juveniles increasingly resembled the thorny appearance of adults as they aged (Figs. 1, 4b and 5). The transition to a dominance of pointed spines was gradual and variable among individuals of similar sizes and ages. When they first appeared, the pointed spines were similar in colour to the body (opaque pink-white). These spines were located around the arms, along the edges and towards the ambulacral groove (Figs. 2 and 5). The largest pointed spines were those along the sides of arms. By 90 days post-settlement, the juveniles had an average of 1.53 (SE = 0.15, $n = 34$) pointed spines per arm, increasing linearly with age (est. = 0.038 ± 0.01 SE, $df = 218.28$, $t = 32.984$, $p = < 0.001$, $n = 263$, $R^2_{Marginal} = 0.822$; Fig. 4b) to a mean of 9.81 (SE = 0.31, $n = 30$) by 300 days.

The transition to adult-like spines began with the lengthening of pointed spines on the sides of arms. These spines took on a yellow-orange hue in individuals of approximately 6 mm diameter, as observed by Yamaguchi (1973). The two marginal spines closest to the terminal tentacle groove became opaque and began to lengthen, transitioning to a diamond-like shape (Fig. 5). These spines continued to lengthen as the juveniles aged, converging on the appearance of the pointed spines and conveying a horn-like appearance at the arm tip ('arm tip' spines; Fig. 5). It seemed that these marginal spines transitioned to the structure of a pointed spine, although it is also possible that they dropped off and were replaced. As the pair of pointed spines at the tip of the arms developed, more pointed spines appeared on the sides of arms and around the growth zone, and those along the sides of the arms lengthened. Pointed spines also began to

Table 1 Model specifications and statistics for GAMMs exploring relationships between morphological traits and time as a smooth predictor. *k*: basis dimension; edf: effective degrees of freedom; F: F-statistic. Note: edf = reference edf in all cases. Traits with edf ~ 1 were subsequently modelled using linear mixed effects models

Trait	*k*	Response Distribution	edf	F	*n*	*p-value*
Total diameter (mm)	4	Gaussian	2.61	1746	317	< .001
Number of arms	4	Quasipoisson	2.96	956.4	317	< .001
Number of pointed spines (/arm)	3	Gaussian	1.40	759.5	263	< .001
Number of marginal spines (/arm)	3	Gaussian	1.97	60.44	263	< .001
Average arm length (mm)	3	Gaussian	1.04	1288	235	< .001
Central disk diameter (mm)	3	Gaussian	1.94	882.4	237	< .001
Mouth diameter (mm)	4	Gaussian	2.63	309.1	235	< .001

form on the aboral surface of the arm toward the end of the study (Fig. 5).

At 90 days post-settlement, the mean diameters of the central disk and mouth were 1.78 mm (SE = 0.08, $n = 33$, range 0.94–2.68 mm) and 0.87 mm (SE = 0.04, $n = 34$, range 0.49–1.28 mm), respectively. The growth patterns of the central disk (edf = 1.94; Fig. 3d, Table 1) and mouth (edf = 2.63; Fig. 3e, Table 1) diameters were monotonic positive but decreased marginally in growth rate toward the end of the study. Central disk diameter increased to an average of 5.96 mm (SE = 0.09, $n = 30$, range 5.30–6.88 mm) by 300 days post-settlement, while mouth diameter averaged 2.47 mm (SE = 0.05, $n = 30$, range 2.08–2.97 mm).

In general, variation across traits was lowest in the earlier months and increased with age (Figs. 3 and 4).

Modelling juvenile age with respect to changes in morphological traits

We used two combinations of traits: (1) total diameter, marginal spines, arm buds), and (2) pointed spines, marginal spines, arms, arm buds), to fit models containing all subset combinations of trait predictors to explore their use as an aging tool for the juveniles. Total diameter and the number of arms traits were multicollinear and could not be included in the same model. Similarly, pointed spines, total diameter, central disk diameter, mouth diameter and arm length traits exhibited multicollinearity and could not be included as predictors in a single model (see methods).

From the total diameter trait set (total diameter, marginal spines, arm buds), Model 1, containing the three trait predictors, explained the largest percentage of variance with respect to age ($R^2_{marg} = 0.904$; Tables 2, 3; Fig. 6). This model also presented a high AIC_{wt} (0.797), supporting this as the best candidate model as indicative of age, marginally outperforming total diameter alone (Table 2). Standardised coefficients of Model 1 revealed that total diameter exhibited a much stronger linear strength of effect on age than that of the marginal spines and arm buds (Table 3B).

From the pointed spines trait set (number of pointed spines, marginal spines, arms and arm buds), the model (Model 8) containing the four traits explained the largest percentage of total variance with respect to age ($R^2_{marg} = 0.870$; Tables 4, 5; Fig. 7.) of all candidate models. This model also exhibited a high AIC_{wt} (0.944), suggesting this was the best candidate model as indicative of age (Table 4). There was little support for all other candidate models ($AIC_{wt} \sim 0$; Table 4). Standardised regression coefficients of Model 8 indicated that the number of pointed spines was the strongest single predictor of age, followed by the number of arms, number of marginal spines, and number of arm buds, respectively (Table 5B). Importantly, models (Model 8; $R^2_{marg} = 0.870$, Table 4) containing a combination of morphological trait predictors explained comparable variance with respect to age as that of total diameter alone (Model 4; $R^2_{marg} = 0.896$; Table 2). As diameter has been widely used to describe growth in COTS juveniles our findings support the use of a combination of morphological traits as an indicator of age.

Growth model fitting

The functions for each of the growth models examined are shown in Table 6, with the Gompertz being the best supported (Table 6). For the Gompertz model, the age and size of inflection, where growth reached a maximum and then slowed, were determined to be 167.5 days (~ 5.5 months) and 4.5 mm, respectively. The maximum growth rate was determined to be 0.033 mm day^{-1} to an asymptotic size of 12.2 mm. The Gompertz, exponential, linear and logistic growth curves are shown in the Supplementary Material (Online Resource S2).

Discussion

The early juvenile stages of benthic marine invertebrates are difficult to study as they often live in cryptic habitats, as

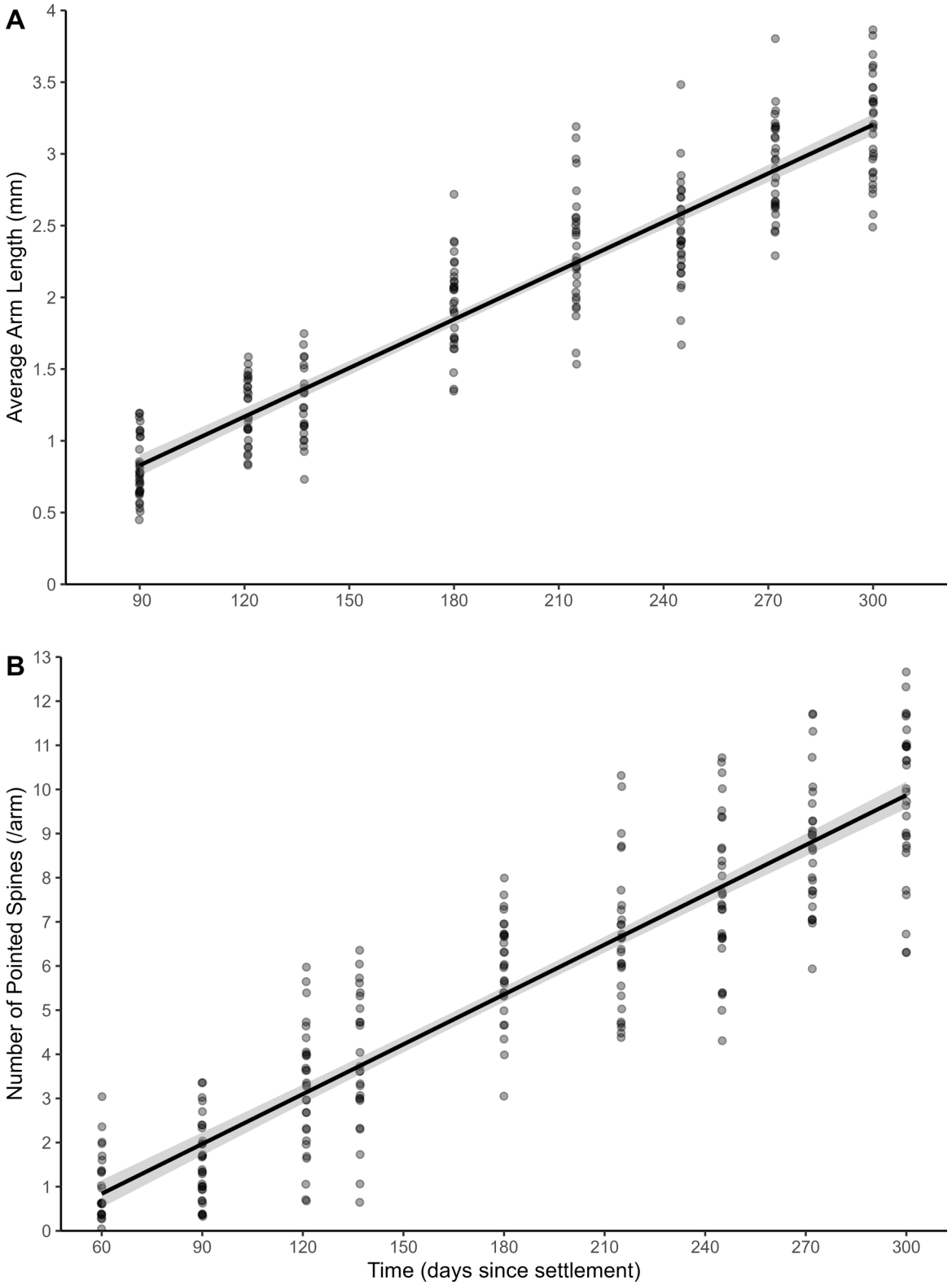

Fig. 4 Linear mixed effects models of relationships between **A** average arm length and **B** number of pointed spines per arm in juveniles to 300 days age. Points are individual observations ($n = 235$ and 263 for arm length and pointed spines, respectively). Data points are jittered to avoid overplotting (one-day axis breaks; width = 0.15, height = 0). Grey shading, 95% confidence interval

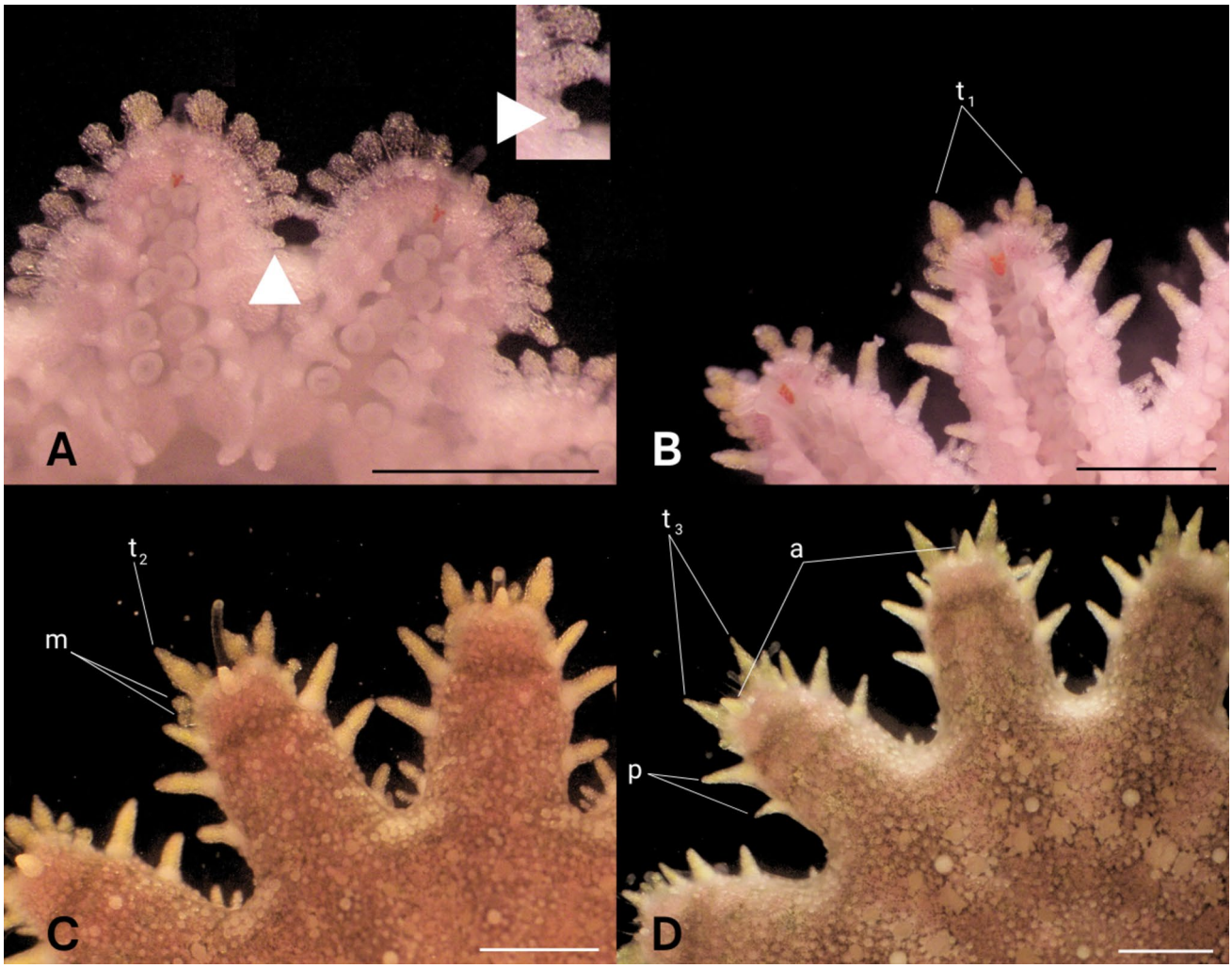

Fig. 5 Development of pointed (p) and 'arm tip' (t) spines in early (**A**) and older (**B, C, D**) juvenile COTS. **A, B** Oral surface. **C, D** Aboral surface. p, pointed spines. t_1, spines in the growth zone have a diamond-like shape; t_2, elongation of diamond-like spines; t_3, convergence of 'arm tip' spines with appearance of pointed spines with growth. m, marginal spines in older juvenile; a, pointed spines on aboral surface. White arrowheads indicate pointed spines in an early juvenile (see inset). Scale bars indicate 1 mm

Table 2 Model selection table to compare morphological trait models used to predict juvenile age. The traits include: total diameter (TDiam), number of marginal spines per arm (MaSpines) and number of arm buds (nBuds). As spine data could only be collected from 60 days, models incorporate data from 60 to 300 days post-settlement. 'Predictors' refers to the combination of explanatory variables included in each model. ΔAIC is the difference in AICC between the candidate model and the model with the lowest AICC. AICwt is the AIC weight, the probability that the model represents the best of all candidate models obtained from this dataset (according to AIC). R2conditional describes the variance explained by both fixed and random factors, whereas R2marginal describes variance explained by fixed effects alone. Parameters with a significant slope are highlighted in bold. The five best models are presented. n = 261

Model Number	Predictors	AIC_C	ΔAIC	AIC_{wt}	$R^2_{conditional}$	$R^2_{marginal}$
1	TDiam, MaSpines, nBuds	2407.6	0.00	0.797	0.944	0.904
2	TDiam, MaSpines	2410.4	2.83	0.193	0.944	0.902
3	TDiam, nBuds	2416.5	8.97	0.009	0.942	0.899
4	TDiam	2420.9	13.30	0.001	0.942	0.896
5	nBuds, MaSpines	2833.0	425.45	0.000	0.776	0.427
6	nBuds	2859.5	451.97	0.000	0.786	0.304
7	MaSpines	2907.9	500.29	0.000	0.875	0.068

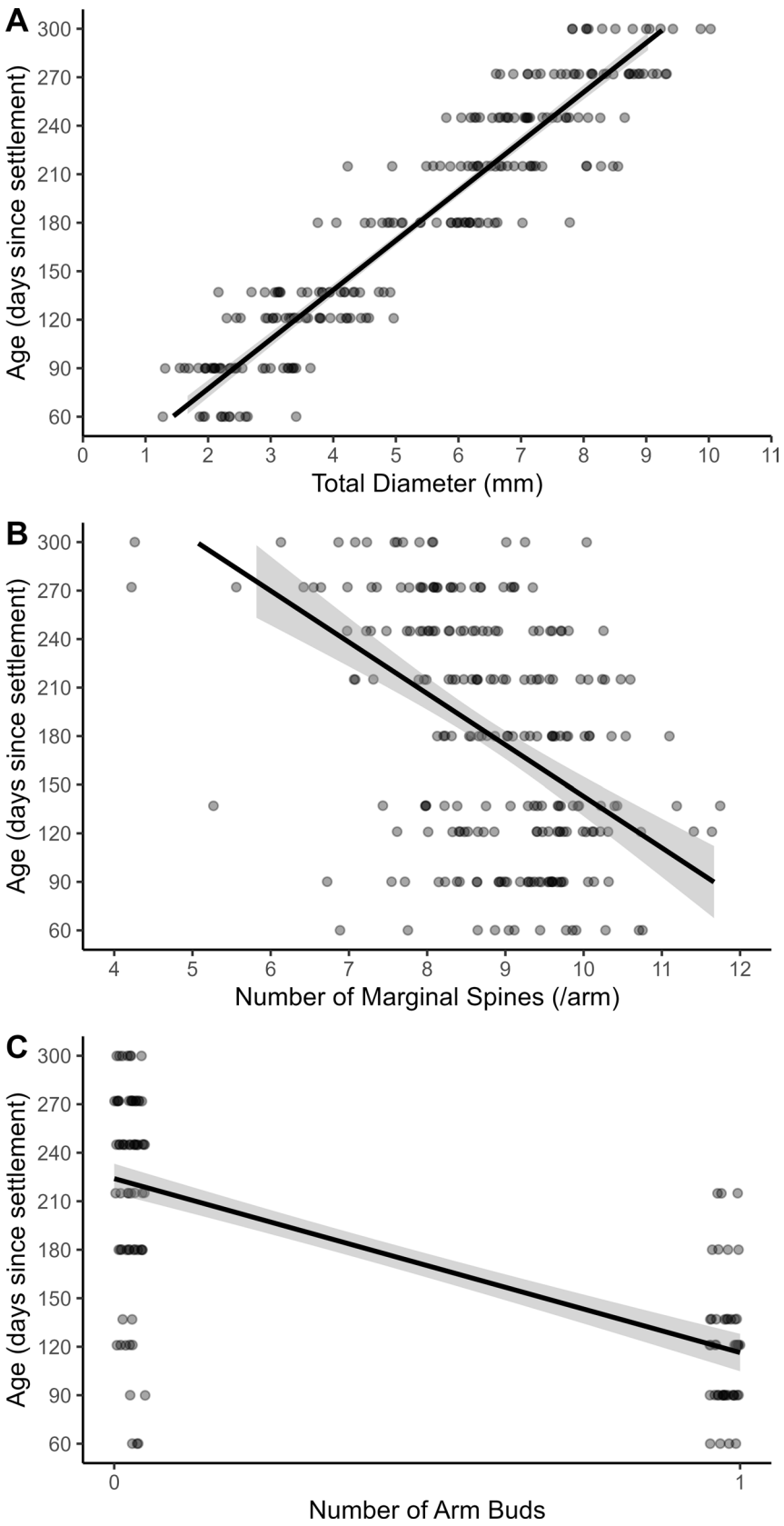

Fig. 6 Linear mixed model (Model 1) including trait predictors, **A** total diameter, **B** the number of marginal spines per arm and **C** the number of arm buds, and juvenile age. As spine data could only be collected from 60 days, the model incorporates data from 60- to 300- days post-settlement. Points are individual observations (n = 261). Data points are 'jittered' to avoid overplotting (single *x*-axis breaks; total diameter, marginal spines: width = 0.15, height = 0.15; arm buds: width = 0.05, height = 0.15). Grey shading, 95% confidence interval

Table 3 Model 1 parameters for linear mixed model testing the effects of morphological traits on juvenile age (see Table 2). A Unstandardised and B standardised model coefficients are presented. Determined using Akaike Information Criterion (AIC) (see methods), this model was the best model constructed from the total diameter (TDiam), marginal spines (MaSpines) and arm bud (nBuds) traits. As spine data could only be collected from 60 days, the model incorporates data from 60- to 300-days post-settlement. Estimates, standard errors (SE), t- and z-statistics, and associated p-values are depicted for each model parameter. n = 261

A				
Parameter	Estimate	SE	*t*	Pr(>|*t*|)
Intercept	74.4072	14.5289	5.121	< .001
TDiam	28.0726	0.8484	33.088	< .001
MaSpines	− 4.7048	1.3994	− 3.362	< .001
nBuds	− 8.9450	4.0082	− 2.232	.03
B				
Parameter	Estimate	SE	*z*	Pr(>|*z*|)
Intercept	182.382	1.608	113.441	< .001
TDiam	68.804	2.079	33.088	< .001
MaSpines	− 5.613	1.670	− 3.362	< .001
nBuds	− 4.365	1.956	− 2.232	.03

is the case for *Acanthaster* sp. (Wilmes et al. 2020b). This life stage is important to understand because juvenile survival and migration to adult habitat are critical demographic processes (Gosselin and Qian 1997; Gillanders et al. 2003). For *Acanthaster* sp. and other predatory sea stars, juvenile habitat and diet can be very different from those of the adults and there can be considerable spatial separation between juvenile nursery areas and adult habitats (Nauen 1978; Zann et al. 1987; Sewell and Watson 1993; Byrne et al. 2021). The vulnerability of post-metamorphic sea stars is shown in high mortality of juvenile *Acanthaster* sp. (Zann et al. 1987; 99% mortality, mostly due to disease) and other sea star species monitored in nature (Sewell and Watson 1993). Juveniles can also remain in the recruitment/nursery habitat with growth stasis for some time, as seen for *Marthasterias glacialis* in nature (6 + years; Byrne et al. 2021) and COTS in captivity (6 + years; Deaker et al. 2020a). This creates an age-size disconnect presenting a challenge for modelling population dynamics of these ecologically important echinoderms.

Herbivorous juvenile COTS are rarely seen in nature despite extensive searches, including destructive sampling efforts (Doherty and Davidson 1988; Birkeland and Lucas 1990), although juveniles were found on a reef flat in Fiji (Zann et al. 1987) and searches on the GBR found juveniles on rubble in forereef habitat (Wilmes et al. 2020a). In the Fiji study, the juvenile population was tracked over two years (Zann et al. 1987). When first encountered they were 10–32 mm diameter and estimated to be 7 months old. Most of them were < 20 mm diameter and living on coralline algae in an area with low coral cover (Zann et al. 1987). Given the size range of the juveniles, the population probably included individuals of mixed diet histories and from multiple cohorts/ages, as well as being older than the nominated age used for the growth analysis in Zann et al. (1987). In the GBR study, juveniles 2–64 mm total diameter (only 2 > 50 mm) were sampled over 8 months (Wilmes et al. 2020a). With the assumption that the juveniles were a single cohort from a summer recruitment date, age (post-spawning) was estimated and used for growth analysis. More than one year class may have been present (Wilmes et al. 2020a). In both field studies, the large size range of the herbivorous stage juveniles present and the presence of large juveniles

Table 4 Model selection table to compare morphological trait models used to predict juvenile age. The traits include: average number of pointed spines per arm (PSpines), average number of marginal spines per arm (MaSpines), number of arms (nArms) and number of arm buds (nBuds). As spine data could only be collected from 60 days, models incorporate data from 60- to 300-days post-settlement. 'Predictors' refers to the combination of explanatory variables included in each model. ΔAIC is the difference in AICC between the candidate model and the model with the lowest AICC. AICwt is the AIC weight, the probability that the model represents the best of all candidate models obtained from this dataset (according to AIC). R2conditional describes the variance explained by both fixed and random factors, whereas R2marginal describes variance explained by fixed effects alone. Parameters with a significant slope are highlighted in bold. The five best models are presented. n = 261

Model number	Predictors	AIC_C	ΔAIC	AIC_{wt}	$R^2_{conditional}$	$R^2_{marginal}$
8	PSpines, MaSpines, nArms, nBuds	2456.6	0.00	0.944	0.961	0.870
9	PSpines, MaSpines, nArms	2462.2	5.66	0.056	0.960	0.865
10	PSpines, nArms, nBuds	2477.0	20.45	0.000	0.961	0.852
11	PSpines, nArms	2486.3	29.77	0.000	0.961	0.842
12	PSpines, nBuds, MaSpines	2527.7	71.08	0.000	0.929	0.837
13	PSpines,					
nBuds	2532.4	75.83	0.000	0.930	0.830	
14	PSpines, MaSpines	2552.2	95.59	0.000	0.923	0.816
15	PSpines	2559.3	102.71	0.000	0.926	0.804

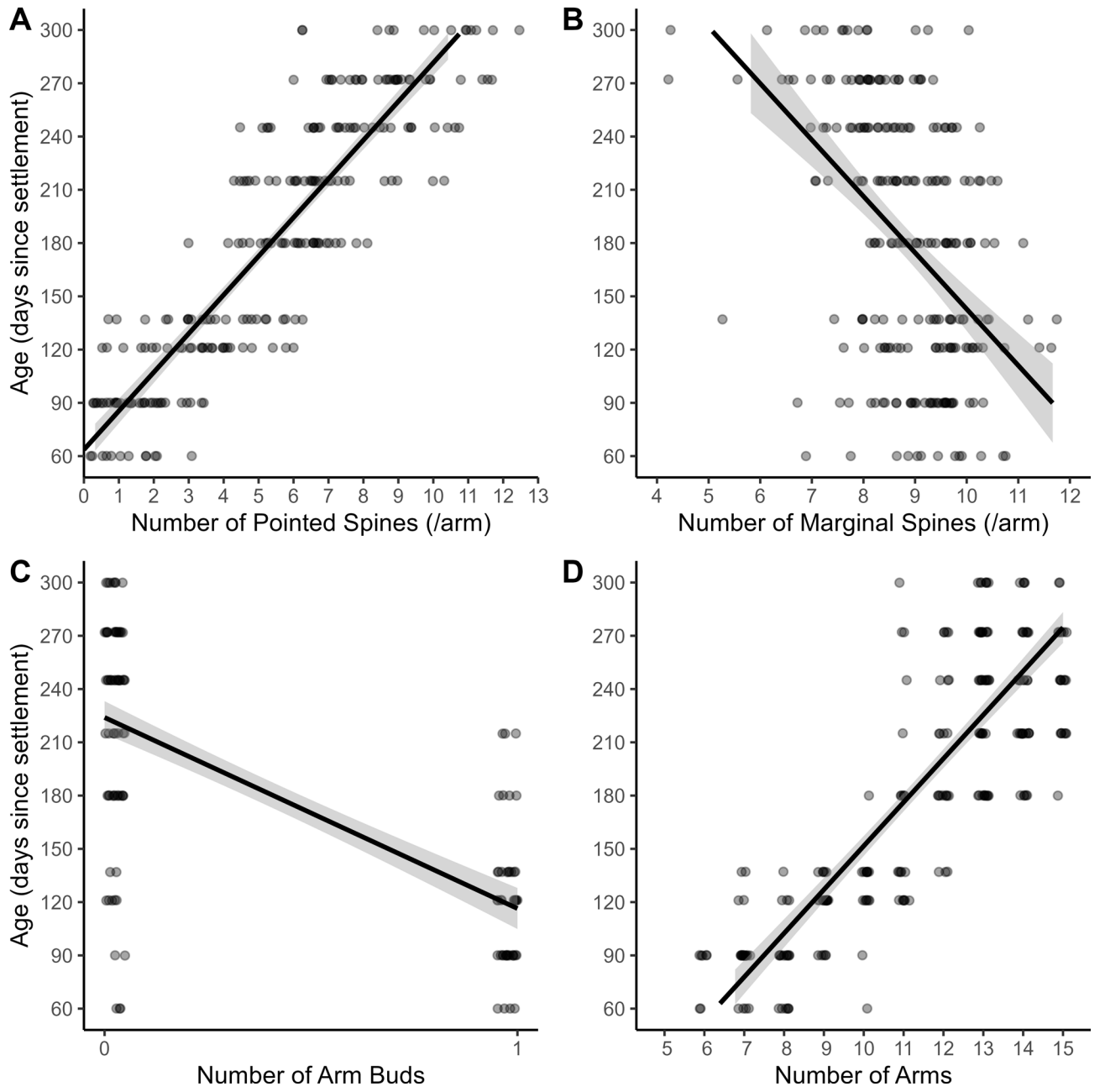

Fig. 7 Linear mixed model (Model 8) including trait predictors, **A** the number of pointed spines per arm, **B** the number of marginal spines per arm, **C** the number of arm buds and **D** the number of arms, and juvenile age. As spine data could only be collected from 60 days, the model incorporates data from 60- to 300- days post-settlement. Points are individual observations ($n = 261$). Data points are jittered to avoid overplotting (single x-axis breaks; pointed spines, marginal spines, arms: width = 0.15, height = 0.15; arm buds: width = 0.05, height = 0.15). Grey shading, 95% confidence interval

(~ 20 mm diameter) living in CCA-coral rubble shows that the size/age of juveniles at the transition to corallivory can be much larger than the ~ 8 mm diameter minimum and that they were likely to be older than the < 1 year estimate in growth models (Wilmes et al. 2020a). Several studies suggest or show that herbivorous juvenile COTS in nature may be several years old (review Birkeland and Lucas 1990).

Unless juvenile populations are monitored from settlement, as in serendipitous encounters in nature (Byrne et al. 2021) or through ex situ rearing, it is difficult to quantify cohort age and model growth dynamics, especially due to the growth plasticity of juvenile sea stars and their potential for growth stasis. We documented growth of a large population of juvenile COTS to 300 days post-settlement

Table 5 Model 8 parameters for linear mixed model testing the effects of morphological traits on juvenile age (see Table 4). A Unstandardised and B standardised model coefficients are presented. Determined using Akaike Information Criterion (AIC) (see methods), this model was the best model constructed from the pointed spines (PSpines), marginal spines (MaSpines), arm number (nArms) and arm bud (nBuds) traits. As spine data could only be collected from 60 days, the model incorporates data from 60- to 300-days post-settlement. Estimates, standard errors (SE), t- and z-statistics, and associated p-values are depicted for each model parameter. n = 261

A				
Parameter	Estimate	SE	*t*	Pr(>|*t*|)
Intercept	74.1273	15.9842	4.638	< .001
PSpines	12.2098	0.8969	13.613	< .001
MaSpines	− 7.5539	1.5449	− 4.890	< .001
nArms	10.0116	1.0657	9.395	< .001
nBuds	− 11.5409	4.1076	− 2.810	.006
B				
Parameter	Estimate	SE	*z*	Pr(>|*z*|)
Intercept	182.672	1.902	96.035	< .001
PSpines	40.092	2.945	13.613	< .001
MaSpines	− 9.012	1.843	− 4.890	< .001
nArms	27.297	2.906	9.395	< .001
nBuds	− 5.632	2.004	− 2.810	.006

Table 6 Fitted model types, growth curves and residual sum of squares (RSS) values for growth curves explaining the relationship between total diameter (TD) and age (days) of COTS juveniles from seven- to 300- days post-settlement

Model Type	Equation	RSS
Gompertz	$TD = 12.1894^{-3.0144^{-0.0073*age}}$	159.8
Exponential	$TD = 70.70^{0.0004*age} - 70.450$	163.4
Linear	$TD = 0.0290 * age + 0.17\,0$	164.0
Logistic	$TD = \frac{9.7572}{(1+10.9859^{-0.0147*age})}$	164.8

and so were able to quantify growth traits in individuals of known age. Previous studies of juvenile COTS from settlement quantified total diameter and arm addition in a small number ($n = 6$–14) of juveniles (Yamaguchi 1973, 1974; Lucas 1984). As expected, the diameter and the number of arms of the juveniles that we reared, were associated with age. We undertook a new approach to quantify growth in juvenile COTS from settlement, using these and previously unexplored (e.g. spine type and number) traits. Our findings supported our hypothesis that a suite of traits is strongly associated with age and indicated that combinations of traits can be used to determine the age of juvenile COTS. The ability to track and model the changes in growth in juveniles of known age complements the models generated for growth of juveniles collected in the field where age was estimated (Wilmes et al. 2020a). Our results indicate that the use of a combination of morphological traits is a promising approach to model juvenile age in *Acanthaster* sp. Eight traits were explored to assess their potential as indicators of age. Avoiding multicollinearity, we identified two groups of traits for analysis. Within their respective groups, diameter and the number of pointed spines were the strongest linear predictors of age across all traits.

In the first trait group, the total diameter trait had the strongest linear effect on age and was much stronger than the marginal spines and arm bud traits. The strength of total diameter as a predictor of age is clear when food is not limited and conditions are stable, as in this study, but variable food conditions may compromise its use as an age indicator in the field (Deaker et al. 2020a). The juveniles reared in this study did not reach the size plateau on an algal diet (Deaker et al. 2020b) but the beginnings of a plateau was indicated when growth began to slow. The strength of the total diameter trait would decrease at the point in which growth stasis was reached.

In the second trait group, the number of pointed spines trait had the strongest linear effect on age followed by the number of arms, marginal spines and arm buds. The pointed spines trait as a predictor of age was stronger in effect than the number of arms. The strength of this trait was likely due to the consistent formation of new spines as the arms grew, as well as their appearance on the aboral surface with growth. These spines are a major feature of COTS and may be a good indicator of age as they appear to be added in a regular pattern. In early juveniles, pointed spines grew on the sides of arms, lengthening with age. These may represent the first signs of the latero-oral spines described for adults (Motokawa 1986). Large spines began to appear on the aboral body wall of the juveniles toward the end of our study.

Although the juveniles were reared in similar conditions, there was considerable variability in their development and pace of growth. Our measurements were taken in juveniles from two genetically different sources (parents) and so we cannot attribute variability to genotypic or phenotypic differences among individuals. Cohorts of post-metamorphic echinoderms can show considerable interindividual variability in growth rates (Lawrence and Lane 1982). Variable growth may have been influenced by size at metamorphosis. Some of the newly metamorphosed COTS we reared were almost twice the size of their clutch mates (Byrne, pers obs). This variation is important in nature where growth rates and survival are often determined by the size of the post-larval juvenile (Gosselin and Qian 1997), often attributed to latent or carry over effects from the larval stage (Pechenik et al. 1998). The importance of size/age dependant mortality has been shown for COTS (Keesing and Halford 1992; Keesing et al. 2018).

Growth of juvenile COTS is strongly influenced by temperature and diet (Yamaguchi 1973; Lucas 1984; Kamya et al. 2016; Deaker et al. 2020b). Growth is faster on a diet of CCA than on *Amphiroa* (Deaker et al. 2020b). The seven juveniles reared at 27–28 °C on a CCA diet by Yamaguchi (1973, 1974) reached the 8 mm size limit to transition to coral at 4 months post-settlement and reached a terminal number of 16–18 arms by 4.5 months. A slower growth was recorded by Lucas (1984) in nine juveniles reared at 21–27 °C (mean 24.5 °C) on a CCA diet. These juveniles achieved 8 mm diameter at ~ 7 months. In a subsequent study of juveniles reared in similar conditions, at one, four, and seven months of age they had mean diameters of 1.0, 2.8 and 4.9 mm, respectively (Keesing and Halford 1992), similar to the present study. The juveniles we reared at 25–26 °C and fed *Amphiroa* sp. reached 8 mm diameter at seven months, although this was variable (4.3–8.6 mm TD). A population mean of 8 mm diameter was not reached until nine months with a maximum of 15 arms. Our juveniles did not reach a size plateau (see Deaker et al. 2020b) but may have done so if we extended our rearing for a few months.

Variability in growth of juvenile COTS in response to external factors such as temperature and food availability (Kamya et al. 2016; Deaker et al. 2020b), as well as their ability to undergo long periods of growth stasis (Deaker et al. 2020a), presents a major challenge in generalising the use of combinations of morphological traits as indicators of age in field-caught individuals. Growth following the transition to coral is also highly variable depending on juvenile age and the coral species provided (Neil et al. 2020). Moreover, it is not known if growth stasis in advanced herbivorous juveniles impacts the development of other morphological traits. Despite approaching a size plateau on a diet of *Amphiroa* sp., the pointed spines continued to be added at the same rate, even following the decline in growth rate. If the spines are added regularly through periods of growth stasis and are independent of size, they would have potential as an age marker for populations in the field. The role that phenotypic plasticity might play in the development of morphological traits requires further consideration. It will be important to determine if the formation and growth of the pointed spines is influenced by growth stasis, in a setting where a variety of algae is provided reflecting potential food sources in nature. Similarly, exploration of a range of traits under different laboratory treatments (e.g. diet and temperature) would be useful to determine their potential to be used as indicators of age.

The number of arm buds and marginal spines were negatively associated with age as these are early juvenile traits, with the spines used for attachment (Yamaguchi 1973). The appearance of arm buds in the first month heralds new arm development. Arm addition decreased by seven months. The fate of the marginal spines was not clear. Their decrease with age indicates that some marginal spines were lost or resorbed with some evidence that they may transition to become pointed spines. In older juveniles, pointed spines appeared in the growth zone where some of the original marginal spines were located. The marginal spines may be replaced by pointed spines.

As the juveniles aged, they changed from stellate five-armed stars to a disk shape as the central disk became dominant. This body form transition and disproportionate growth of the disk is unusual compared with other predatory sea stars and is a specialised trait for corallivory (Byrne et al. 2024b). The disk grew to extend over the basal region of the aboral side of the arms. As a result, only a portion of the actual arm length was evident on aboral view. Thus, we used oral arm length as a better reflection of true arm length. We recommend use of the oral side arm measure for COTS as arm length is a key trait used to characterise growth in sea stars. Other studies of COTS have measured the arms on aboral view (e.g. Deaker et al. 2021a).

The large mouth of the juveniles allows for eversion of the stomach over algae creating feeding scars that approximate the size of the central disk (Deaker and Byrne 2022). The distinct disk profile that the juveniles develop foreshadows the large central body of the future corallivorous adult which accommodates their voluminous, unusually large cardiac stomach (Jangoux 1982), as well as substantial nutritive storage organs (Lawrence and Moran 1992). In adult COTS, the flattened disk-shape enables a large food intake capacity relative to maintenance requirements (Birkeland and Lucas 1990).

Toxic spines are a distinct feature of COTS compared to other sea stars and indicate that there has been selection for protection against predators. This defensive capacity undoubtedly contributes to their success. As a unique feature of COTS, the biology of the spines is of interest to explore. While our results suggest that the pointed spines trait may serve as an age marker, their development in the field may be a plastic character. For instance, plasticity of defensive morphology in response to predator cues has been observed in the addition of byssal threads in bivalves (e.g. Garner and Litvaitis 2013), enhanced retractability in gastropods (e.g. Miner et al. 2013) and longer spines in bryozoans (e.g. Harvell 1998). In the green sea urchin *Stronglyocentrotus droebachiensis*, larvae exposed to crab effluent produce post-settlement juveniles with more spines (Barnes and Allen 2023). The juveniles respond behaviourally to cues from crabs and adult conspecifics in a strong avoidance response (Deaker et al. 2021b; Webb et al. 2024), a sensory ability that may also promote anti-predator phenotypic plasticity. It is not known if exposure to predator cues as larvae or juveniles would influence spine development in juvenile COTS. Exposing the juveniles to the chemistry of their decorator crab predators (Desbiens et al. 2023) to see if this promotes

an increase in toxin production or influences spine development is a topic deserving of additional research. Understanding these processes will be important in future interpretation of morphological traits, in particular pointed spines, as indicators of age in the field. The spines have also been used to age adult COTS using the pigment bands that develop along the shaft and which appear to be formed periodically (Stump and Lucas 1990). Thus, the spines may provide insight into the biology and ecology of COTS as an age marker across multiple life stages. The importance of pointed spine development as a potential age marker for juvenile and adult COTS warrants attention.

Several studies have used a range of functions to fit growth curves to estimate age-size relationships of COTS (Lucas 1984; Zann et al. 1987; Deaker et al. 2020a; Wilmes et al. 2020a). The two studies that used data from juveniles sampled in the wild applied an estimated spawning date to predict month of settlement to estimate age for analysis. The field setting of these studies and inability to follow an identified cohort from settlement makes it impossible to determine exact age. Conditions such as variable diet, availability of coral prey and especially the timing of transition to coral strongly influences growth in juvenile COTS (Deaker et al. 2020a; Wilmes et al. 2020a). While this makes it difficult to compare the growth models fitted from field-based data with those determined here for known age herbivorous juveniles, there is overall support for application of the Gompertz model with the age of inflection approximating the age/size at which growth slows on an algal diet (in the absence of coral prey) and juveniles are competent to switch to a coral diet. Changes in early post-settlement growth in marine invertebrates are often associated with shifts in diet and for COTS this is marked in association with the switch from CCA to coral prey (Birkeland and Lucas 1990; Wilmes et al. 2020a).

Modelling of size-at-age suggests that juvenile growth over the first 10 months was non-linear, with a decrease in growth at 5–6 months. Wilmes et al. (2020a) proposed a switch from a CCA to coral diet starting at ~ 6 months at a threshold size of 8–10 mm, with < 10% of juveniles feeding on coral by 10 months (> 50% by 11 months). These characteristics are consistent with that determined here, with growth inflection occurring at ~ 5 to 6 months (when the juveniles were 5–6 mm in diameter), and asymptotic (limited) growth becoming apparent toward the end of our study when the juveniles were ~ 8 to 10 mm diameter.

Our Gompertz growth model predicts an average asymptotic size of 12.2 mm, similar to that seen by Wilmes et al. (2020a), where over 90% of field-collected juveniles were still feeding on CCA at a median diameter of 12–13 mm. Our findings of growth to an asymptotic size in juveniles fed coralline algae are also consistent with the laboratory study of Deaker et al. (2020a). The growth trajectories of juveniles on CCA (Deaker et al. 2020a) are also consistent with our Gompertz model, with a maximum growth rate around 100 days (80–120 days) and growth decreasing around 200 days. This slowing of growth around 8 mm diameter in juveniles reared on *Amphiroa* for their entire life indicates that additional growth on this single diet would be reduced, perhaps due to energetic limitations. Juvenile growth rates are strongly influenced by the quality of the algal diet provided (Deaker et al. 2020b). Interestingly, after 6.5 years juveniles on a CCA diet had growth stasis around ~ 18 mm diameter, while Wilmes et al. (2020a) found much larger juveniles on CCA in the field.

The juvenile stage of COTS is a black box in our understanding of outbreaks, impeded by a lack of data on recruitment, settlement, mortality and growth rates (Wilmes et al. 2018). The ability to age juvenile COTS is critical to understanding post-settlement processes and is needed to inform population models seeking to understand their role in driving COTS outbreaks. This study addresses knowledge gaps on juvenile COTS to inform age modelling using morphological traits, thereby contributing to the understanding of the biology and ecology of this cryptic life stage. Our results may inform estimates of the age of juveniles found in nature.

Acknowledgements We thank the staff of the Sydney Institute of Marine Science (SIMS) for assistance in maintaining the adults. The COTS Control Team are thanked for collecting the adults. We thank the reviewers for their insightful comments which improved the manuscript. This is SIMS contribution number 315.

Author contributions Liam Wilson and Maria Byrne designed the study and wrote the manuscript. Liam Wilson did all the material preparation, data collection and analysis. Thomas White and Miles Lamare advised on the statistics and modelling. Paulina Selvakumaraswamy reared the larvae and generated photography data. All authors read and approved the final manuscript.

Funding Open Access funding enabled and organized by CAUL and its Member Institutions. Funding support was provided by the COTS Control Innovation Program, which is funded by the partnership between the Australian Government's Reef Trust and the Great Barrier Reef Foundation.

Data availability Data will be placed in the University of Sydney data repository (Sydney eScholarship Repository) and made available upon publication with an open access link.

Declarations

Conflict of interest The authors have no relevant financial or non-financial interests to disclose.

Ethical approval No approval of research ethics committees was required to accomplish the goals of this study as work was conducted with an unregulated invertebrate species.

References

Australian Institute of Marine Science (2023) Daily average ocean water temperatures against long term average water temperature. https://data.aims.gov.au/aimsrtds/yearlytrends.xhtml. Accessed 15 Mar 2023

Barnes DK, Allen JD (2023) Predators induce phenotypic plasticity in echinoderms across life history stages. Biol Bull 244:103–114. https://doi.org/10.1086/725633

Barton K (2023) MuMIn: Multi-model inference. R Project CRAN. https://CRAN.R-project.org/package=MuMIn. Accessed 17 Mar 2023

Birkeland C (1982) Terrestrial runoff as a cause of outbreaks of *Acanthaster planci* (Echinodermata: Asteroidea). Mar Biol 69:175–185. https://doi.org/10.1007/Bf00396897

Birkeland C, Lucas JS (1990) *Acanthaster planci*: Major management problem of coral reefs. CRC Press, Boca Raton

Bozec Y-M, Hock K, Mason RAB, Baird ME, Castro-Sanguino C, Condie SA, Puotinen M, Thompson A, Mumby PJ (2022) Cumulative impacts across Australia's Great Barrier Reef: a mechanistic evaluation. Ecol Monogr 92:e01494. https://doi.org/10.1002/ecm.1494

Byrne M, Minchin D, Clements M, Deaker DJ (2021) The waiting stage, prolonged residency in nursery habitats by juveniles of the predatory sea star *Marthasterias glacialis*. Biol Bull 241:219–230. https://doi.org/10.1086/715843

Byrne M, Deaker DJ, Gibbs M, Selvakumaraswamy P, Clements M (2023) Juvenile waiting stage crown-of-thorns sea stars are resilient in heatwave conditions that bleach and kill corals. Glob Chang Biol 29:6493–6502. https://doi.org/10.1111/gcb.16946

Byrne M, Foo SA, Vila-Concejo AV, Wolfe K (2024a) Impacts of climate change stressors on the Great Barrier Reef. In: Wolanski E, Kingsford MJ (eds) Oceanographic Processes of Coral Reefs, 2nd edn. CRC Press, Boca Raton, pp 323–340

Byrne M, Clements MJ, Hill RT, Selvakumaraswamy P, Webb MS, Wilson LJ (2024b) Body form transition in the juvenile crown-of-thorns sea star from the 5-armed metamorphosed juvenile to the multi-armed body dominated by the central disk. Cah Biol Mar 65:307–317. https://doi.org/10.21411/CBM.A.6570FD75

Clements M, Selvakumaraswamy P, Deaker D, Byrne M (2022) Freshening of great barrier reef waters is deleterious for larval crown-of-thorns starfish, counter to the terrestrial runoff hypothesis. Mar Ecol Prog Ser 696:1–14. https://doi.org/10.3354/meps14150

Colgan MW (1987) Coral reef recovery on Guam (Micronesia) after catastrophic predation by *Acanthaster planci*. Ecology 68:1592–1605. https://doi.org/10.2307/1939851

Deaker DJ, Byrne M (2022) Crown of thorns starfish life-history traits contribute to outbreaks, a continuing concern for coral reefs. Emerg Top Life Sci 6:67–79. https://doi.org/10.1042/etls20210239

Deaker DJ, Agüera A, Lin H-A, Lawson C, Budden C, Dworjanyn SA, Mos B, Byrne M (2020a) The hidden army: corallivorous crown-of-thorns seastars can spend years as herbivorous juveniles. Biol Lett 16:20190849. https://doi.org/10.1098/rsbl.2019.0849

Deaker DJ, Mos B, Lin H-A, Lawson C, Budden C, Dworjanyn SA, Byrne M (2020b) Diet flexibility and growth of the early herbivorous juvenile crown-of-thorns sea star, implications for its boom-bust population dynamics. PLoS ONE 15:e0236142. https://doi.org/10.1371/journal.pone.0236142

Deaker DJ, Mos B, Lawson C, Dworjanyn S, Budden C, Byrne M (2021a) Coral defences: the perilous transition of juvenile crown-of-thorns starfish to corallivory. Mar Ecol Prog Ser 665:115–125. https://doi.org/10.3354/meps13660

Deaker DJ, Balogh R, Dworjanyn SA, Mos B, Byrne M (2021b) Echidnas of the sea: the defensive behaviour of juvenile and adult crown-of-thorns sea stars. Biol Bull 241:259–270. https://doi.org/10.1086/716777

Desbiens AA, Mumby PJ, Dworjanyn S, Plagányi EE, Uthicke S, Wolfe K (2023) Novel rubble-dwelling predators of herbivorous juvenile crown-of-thorns starfish (*Acanthaster* sp.). Coral Reefs 42:579–591. https://doi.org/10.1007/s00338-023-02364-w

Doherty PJ, Davidson J (1988) Monitoring the distribution and abundance of juvenile *Acanthaster planci* in the central Great Barrier Reef. In: Proc 6th Int Coral Reef Symp, vol 2, pp 131–136

Done TJ, Potts DC (1992) Influences of habitat and natural disturbances on contributions of massive porites corals to reef communities. Mar Biol 114:479–493. https://doi.org/10.1007/bf00350040

Endean R (1969) Report on investigations made into aspects of the current *Acanthaster planci* (crown of thorns) infestations of certain reefs of the great barrier reef. Brisbane: Fisheries Branch, Department of Primary Industries

Garner YL, Litvaitis MK (2013) Effects of injured conspecifics and predators on byssogenesis, attachment strength and movement in the blue mussel, *Mytilus edulis*. J Exp Mar Biol Ecol 448:136–140. https://doi.org/10.1016/j.jembe.2013.07.004

Gillanders BM, Able KW, Brown JA, Eggleston DB, Sheridan PF (2003) Evidence of connectivity between juvenile and adult habitats for mobile marine fauna: an important component of nurseries. Mar Ecol Prog Ser 247:281–295. https://doi.org/10.3354/meps247281

Gosselin L, Qian P (1997) Juvenile mortality in benthic marine invertebrates. Mar Ecol Prog Ser 146:265–282. https://doi.org/10.3354/meps146265

Great Barrier Reef Marine Park Authority (2017) Great Barrier Reef blueprint for resilience. GBRMPA, Townsville. https://elibrary.gbrmpa.gov.au/jspui/bitstream/11017/3287/1/GBRMPA%20Blueprint%20for%20Resilience%20-%20Low%20Res.pdf. Accessed 20 Mar 2023

Greenwell BM, Schubert Kabban CM (2014) Investr: an R package for inverse estimation. R J 6:90–100. https://doi.org/10.32614/RJ-2014-009

Harvell CD (1998) Genetic variation and polymorphism in the inducible spines of a marine bryozoan. Evolution 52:80–86. https://doi.org/10.1111/j.1558-5646.1998.tb05140.x

Haszprunar G, Vogler C, Wörheide G (2017) Persistent gaps of knowledge for naming and distinguishing multiple species of crown-of-thorns-seastar in the *Acanthaster planci* species complex. Diversity 9:22. https://doi.org/10.3390/d9020022

Hughes TP, Kerry JT, Álvarez-Noriega M, Álvarez-Romero JG, Anderson KD, Baird AH, Babcock RC, Beger M, Bellwood DR, Berkelmans R et al (2017) Global warming and recurrent mass

bleaching of corals. Nature 543:373–377. https://doi.org/10.1038/nature21707
Jangoux M (1982) Digestive systems: Asteroidea. In: Jangoux M, Lawrence JM (eds) Echinoderm nutrition, 1st edn. CRC Press, Boca Raton, pp 235–272
Johansson CL, Francis DS, Uthicke S (2016) Food preferences of juvenile corallivorous crown-of-thorns (*Acanthaster planci*) sea stars. Mar Biol 163:49. https://doi.org/10.1007/s00227-016-2823-0
Kamya PZ, Byrne M, Graba-Landry A, Dworjanyn SA (2016) Near-future ocean acidification enhances the feeding rate and development of the herbivorous juveniles of the crown-of-thorns starfish, *Acanthaster planci*. Coral Reefs 35:1241–1251. https://doi.org/10.1007/s00338-016-1480-6
Kayal M, Vercelloni J, Lison de Loma T, Bosserelle P, Chancerelle Y, Geoffroy S, Stievenart C, Michonneau F, Penin L, Planes S et al (2012) Predator crown-of-thorns starfish (*Acanthaster planci*) outbreak, mass mortality of corals, and cascading effects on reef fish and benthic communities. PLoS ONE 7:e47363. https://doi.org/10.1371/journal.pone.0047363
Keesing J, Halford A (1992) Importance of postsettlement processes for the population dynamics of *Acanthaster planci* (L.). Mar Freshw Res 43:635–651. https://doi.org/10.1071/MF9920635
Keesing J, Halford A, Hall K (2018) Mortality rates of small juvenile crown-of-thorns starfish *Acanthaster planci* on the Great Barrier Reef: implications for population size and larval settlement thresholds for outbreaks. Mar Ecol Prog Ser 597:179–190. https://doi.org/10.3354/meps12606
Kroon FJ, Barneche DR, Emslie MJ (2021) Fish predators control outbreaks of crown-of-thorns starfish. Nat Commun 12:6986. https://doi.org/10.1038/s41467-021-26786-8
Kroon FJ, Crosswell JR, Robson BJ (2023) The effect of catchment load reductions on water quality in the crown-of-thorn starfish outbreak initiation zone. Mar Pollut Bull 195:115255. https://doi.org/10.1016/j.marpolbul.2023.115255
Kuznetsova A, Brockhoff PB, Christensen RHB (2017) lmerTest package: tests in linear mixed effects models. J Stat Softw 82:1–26. https://doi.org/10.18637/jss.v082.i13
Lawrence JM, Lane JM (1982) The utilization of nutrients by post-metamorophic echinoderms. In: Jangoux M, Lawrence JM (eds) Echinoderm nutrition, 1st edn. CRC Press, Boca Raton, pp 331–371
Lawrence JM, Moran PJ (1992) Proximate composition and allocation of energy to body components in *Acanthaster planci* (Linnaeus) (Echinodermata: Asteroidea). Zoolog Sci 9:321–328
Lucas JS (1984) Growth, maturation and effects of diet in *Acanthaster planci* (L.) (Asteroidea) and hybrids reared in the laboratory. J Exp Mar Biol Ecol 79:129–147. https://doi.org/10.1016/0022-0981(84)90214-4
Lüdecke D (2018) ggeffects: Tidy data frames of marginal effects from regression models. J Open Source Softw 3:772. https://doi.org/10.21105/joss.00772
Lüdecke D, Ben-Shachar MS, Patil I, Waggoner P, Makowski D (2021) Performance: an R package for assessment, comparison and testing of statistical models. J Open Source Softw 6:3139. https://doi.org/10.21105/joss.03139
Miner BG, Donovan DA, Portis LM, Goulding TC (2013) Whelks induce an effective defense against sea stars. Mar Ecol Prog Ser 493:195–206. https://doi.org/10.3354/meps10501
Motokawa T (1986) Morphology of spines and spine joint in the crown-of-thorns starfish *Acanthaster planci* (Echinodermata, Asteroida). Zoomorphology 106:247–253. https://doi.org/10.1007/BF00312046
Nauen CE (1978) The growth of the sea star, *Asterias rubens*, and its role as benthic predator in Kiel bay. Kieler Meeresforschungen-Sonderheft 4:68–81.
Neil RC, Gomez Cabrera M, Uthicke S (2022) Juvenile age and available coral species modulate transition probability from herbivory to corallivory in *Acanthaster* cf. *solaris* (crown-of-thorns seastar). Coral Reefs 41:843–848. https://doi.org/10.1007/s00338-022-02255-6
Pechenik JA, Wendt DE, Jarrett JN (1998) Metamorphosis is not a new beginning: larval experience influences juvenile performance. Bioscience 48:901–910. https://doi.org/10.2307/1313294
Peharda M, Vilibić I, Black BA, Markulin K, Dunić N, Džoić T, Mihanović H, Gačić M, Puljas S, Waldman R (2018) Using bivalve chronologies for quantifying environmental drivers in a semi-enclosed temperate sea. Sci Rep 8:5559. https://doi.org/10.1038/s41598-018-23773-w
Plagányi ÉE, Babcock RC, Rogers J, Bonin M, Morello EB (2020) Ecological analyses to inform management targets for the culling of crown-of-thorns starfish to prevent coral decline. Coral Reefs 39:1483–1499. https://doi.org/10.1007/s00338-020-01981-z
Pratchett M, Caballes C, Rivera-Posada JA, Sweatman HPA (2014) Limits to understanding and managing outbreaks of crown-of-thorns starfish (*Acanthaster* spp.). In: Hughes RN, Hughes DJ, Smith IP (eds) Oceanography and marine biology: annual review, vol 52. CRC Press, Boca Raton, pp 133–200
Quinn GP, Keough MJ (2002) Experimental design and data analysis for biologists. Cambridge University Press, Cambridge
R Core Team (2024) R: A language and environment for statistical computing. R Foundation for Statistical Computing, Vienna, Austria. https://www.R-project.org/. Accessed 3 March 2023
Schielzeth H (2010) Simple means to improve the interpretability of regression coefficients. Methods Ecol Evol 1:103–113. https://doi.org/10.1111/j.2041-210X.2010.00012.x
Sewell MA, Watson JC (1993) A "source" for asteroid larvae?: recruitment of *Pisaster ochraceus*, *Pycnopodia helianthoides* and *Dermasterias imbricata* in Nootka Sound, British Columbia. Mar Biol 117:387–398. https://doi.org/10.1007/BF00349314
Siegel AF, Wagner MR (2022) Multiple regression: predicting one variable from several others. In: Siegel AF, Wagner MR (eds) Practical business statistics, 8th edn. Academic Press, MA, pp 371–431
Stump RJW, Lucas JS (1990) Linear growth in spines from *Acanthaster planci* (l.) involving growth lines and periodic pigment bands. Coral Reefs 9:149–154. https://doi.org/10.1007/BF00258227
Sun J, Hamel J-F, Gianasi BL, Mercier A (2019) Age determination in echinoderms: first evidence of annual growth rings in holothuroids. Proc R Soc Lond B Biol Sci 286:20190858. https://doi.org/10.1098/rspb.2019.0858
Togashi R, Sakai T (2019) Generalising kendall's tau for noisy and incomplete preference judgements. In: Proc 2019 ACM SIGIR Int Conf Theory Inf Retr, pp 193–196. https://doi.org/10.1145/3341981.3344246
Uthicke S, Schaffelke B, Byrne M (2009) A boom–bust phylum? Ecological and evolutionary consequences of density variations in echinoderms. Ecol Monogr 79:3–24. https://doi.org/10.1890/07-2136.1
Vine PJ (1973) Crown of thorns (*Acanthaster planci*) plagues: the natural causes theory. Atoll Res Bull 166:1–10. https://doi.org/10.5479/si.00775630.166.1
Webb M, Clements M, Selvakumaraswamy P, McLaren E, Byrne M (2024) Chemosensory behaviour of juvenile crown-of-thorns sea stars (*Acanthaster* sp.), attraction to algal and coral food and avoidance of adult conspecifics. Proc R Soc Lond B Biol Sci 291:20240623. https://doi.org/10.1098/rspb.2024.0623
Wickham H (2016) ggplot 2: Elegant graphics for data analysis. Springer, Cham
Wilmes JC, Caballes CF, Cowan Z-L, Hoey AS, Lang BJ, Messmer V, Pratchett MS (2018) Contributions of pre- versus post-settlement processes to fluctuating abundance of crown-of-thorns starfishes

(*Acanthaster* spp.). Mar Pollut Bull 135:332–345. https://doi.org/10.1016/j.marpolbul.2018.07.006

Wilmes JC, Hoey AS, Pratchett MS (2020a) Contrasting size and fate of juvenile crown-of-thorns starfish linked to ontogenetic diet shifts. Proc R Soc Lond B Biol Sci 287:20201052. https://doi.org/10.1098/rspb.2020.1052

Wilmes JC, Schultz DJ, Hoey AS, Messmer V, Pratchett MS (2020b) Habitat associations of settlement-stage crown-of-thorns starfish on Australia's great barrier reef. Coral Reefs 39:1163–1174. https://doi.org/10.1007/s00338-020-01950-6

Wolfe K, Byrne M (2024) Dead foundation species create coral rubble habitat that benefits a resilient pest species. Mar Environ Res 202:106740. https://doi.org/10.1016/j.marenvres.2024.106740

Wolfe K, Graba-Landry A, Dworjanyn SA, Byrne M (2017) Superstars: Assessing nutrient thresholds for enhanced larval success of *Acanthaster planci*, a review of the evidence. Mar Pollut Bull 116:307–314. https://doi.org/10.1016/j.marpolbul.2016.12.079

Wood SN (2003) Thin plate regression splines. J R Stat Soc Series B Stat Methodol 65:95–114. https://doi.org/10.1111/1467-9868.00374

Wood SN (2011) Fast stable restricted maximum likelihood and marginal likelihood estimation of semiparametric generalized linear models. J R Stat Soc Series B Stat Methodol 73:3–36. https://doi.org/10.1111/j.1467-9868.2010.00749.x

Yamaguchi M (1973) Early life histories of coral reef asteroids, with special reference to *Acanthaster planci* (L.). In: Jones OA, Endean R (eds) Biology and geology of coral reefs, vol 2. Academic Press, New York, pp 369–387

Yamaguchi M (1974) Growth of juvenile *Acanthaster planci* (l.) in the laboratory. Pac Sci 28:123–138

Yee TW, Mitchell ND (1991) Generalized additive models in plant ecology. J Veg Sci 2:587–602. https://doi.org/10.2307/3236170

Zann L, Brodie J, Berryman C, Naqasima M (1987) Recruitment, ecology, growth and behavior of juvenile *Acanthaster planci* (L.) (Echinodermata: Asteroidea). Bull Mar Sci 41:561–575